AJNR

Complex Bilobular, Bisaccular, and Broad-Neck Microsurgical Aneurysm Formation in the Rabbit Bifurcation Model for the Study of Upcoming Endovascular Techniques

S. Marbacher, S. Erhardt, J.-A. Schläppi, D. Coluccia, L. Remonda, J. Fandino and C. Sherif

AJNR Am J Neuroradiol 2011, 32 (4) 772-777
doi: https://doi.org/10.3174/ajnr.A2374
http://www.ajnr.org/content/32/4/772

ORIGINAL RESEARCH

Complex Bilobular, Bisaccular, and Broad-Neck Microsurgical Aneurysm Formation in the Rabbit Bifurcation Model for the Study of Upcoming Endovascular Techniques

S. Marbacher
S. Erhardt
J.-A. Schläppi
D. Coluccia
L. Remonda
J. Fandino
C. Sherif

BACKGROUND AND PURPOSE: Despite rapid advances in the development of materials and techniques for endovascular intracranial aneurysm treatment, occlusion of large broad-neck aneurysms remains a challenge. Animal models featuring complex aneurysm architecture are needed to test endovascular innovations and train interventionalists.

MATERIALS AND METHODS: Eleven adult female New Zealand rabbits were assigned to 3 experimental groups. Complex bilobular, bisaccular, and broad-neck venous pouch aneurysms were surgically formed at an artificially created bifurcation of both CCAs. Three and 5 weeks postoperatively, the rabbits underwent 2D-DSA and CE-3D-MRA, respectively.

RESULTS: Mortality was 0%. We observed no neurologic, respiratory, or gastrointestinal complications. The aneurysm patency rate was 91% (1 aneurysm thrombosis). There was 1 postoperative aneurysm hemorrhage (9% morbidity). The mean aneurysm volumes were 176.9 ± 63.6 mm^3, 298.6 ± 75.2 mm^3, and 183.4 ± 72.4 mm^3 in bilobular, bisaccular, and broad-neck aneurysms, respectively. The mean operation time was 245 minutes (range, 175–290 minutes). An average of 27 ± 4 interrupted sutures (range, 21–32) were needed to create the aneurysms.

CONCLUSIONS: This study demonstrates the feasibility of creating complex venous pouch bifurcation aneurysms in the rabbit with low morbidity, mortality, and high short-term aneurysm patency. The necks, domes, and volumes of the bilobular, bisaccular, and broad-neck aneurysms created are larger than those previously described. These new complex aneurysm formations are a promising tool for in vivo animal testing of new endovascular devices.

ABBREVIATIONS: BL = bilobular; BN = broad-neck; BS = bisaccular; CCA = common carotid artery; CE-3D-MRA = contrast-enhanced 3D MRA; DSA = digital subtraction angiography; 2D-DSA = 2D intra-arterial DSA; LCCA = left CCA (p-LCCA = proximal LCCA, d-LCCA = distal LCCA); MRA = MR angiography; RCCA = right CCA; TOF = time-of-flight; VP = venous pouch

Endovascular treatment of small narrow-neck cerebral aneurysms has become an equivalent alternative to microsurgical clipping.[1,2] However, in broad-based and larger aneurysms, recanalization rates are unacceptably high.[3] Additionally, complex aneurysms are at high risk of incomplete occlusion, regrowth, and life-threatening rerupture.[3-5] Thus, animal models featuring such complicated aneurysm geometries are needed to test the long-term stability of new endovascular devices and to train surgeons in highly challenging embolization techniques.

The elastase-induced and the microsurgically produced bifurcation aneurysms are the most frequently used models for testing endovascular devices in rabbits. Although surgical construction of experimental aneurysms is more time-consuming, it allows variation of the anatomy of the bifurcation; aneurysm length; and width, neck size, and neck/sac ratio.[6] Improvements in anesthesia, surgical technique, and peri- and postoperative management have allowed minimization of the major limitations of high mortality and morbidity.[7]

Since the introduction of Guglielmi detachable coils (Boston Scientific, Natick, Massachusetts) at the beginning of the 1990s, there have been numerous attempts to enlarge the field of application from small-neck aneurysms to complex or broad-neck aneurysms. The current armament includes bioactive coils or HydroCoils (MicroVention Terumo, Aliso Viejo, California), 3D coils, liquid embolic agents, balloon-remodeling techniques, microstents, and flow diverters. New endovascular device assessment for the treatment of complex aneurysms is unavoidably linked with in vivo animal testing. However, to our knowledge, descriptions of techniques for the creation of wide-neck aneurysms with complex geometry do not exist. The aim of this study was to demonstrate the feasibility of the creation of aneurysms with complex angioarchitecture by using the venous pouch bifurcation model in rabbits.

Materials and Methods

The study was performed in accordance with the National Institutes of Health guidelines for the care and use of experimental animals and with the approval of the Animal Care and Experimentation Committee of the Canton of Bern, Switzerland (approval number, 112/08).

Received June 19, 2010; accepted after revision August 30.

From the Departments of Intensive Care Medicine (S.M., S.E., D.C., J.F., C.S.) and Neurosurgery (J.-A.S.), Bern University Hospital and University of Bern, Bern, Switzerland; and Department of Neurosurgery (S.M., S.E., D.C., J.F., C.S.) and Division of Neuroradiology (L.R.), Kantonsspital Aarau, Aarau, Switzerland.

This study was supported by the Department of Intensive Care Medicine, Bern University Hospital and University of Bern, Bern, Switzerland, and the Research Fund from the Cantonal Hospital Aarau, Aarau, Switzerland.

Please address correspondence to Serge Marbacher, MD, MSc, Department of Neurosurgery, Kantonsspital Aarau, CH-5000 Aarau, Switzerland; e-mail: serge.marbacher@ksa.ch

DOI 10.3174/ajnr.A2374

Study Design

Eleven adult female New Zealand rabbits weighing 3.0–4.3 kg were assigned to 3 experimental groups. Creation of bilobular, bisaccular, and broad-based aneurysms was performed as described below. Before skin incision, amoxicillin (15 mg/kg; Clamoxyl 25 mg/mL) was given intravenously. All surgical procedures were performed under sterile conditions, and wounds were irrigated thoroughly with neomycin sulfate for infection prophylaxis.

Anesthesia, Clinical Observation, and Sacrifice

Induction of general anesthesia was performed by subcutaneous administration of ketamine hydrochloride (30 mg/kg, Ketalar 50 mg/mL) and xylazine hydrochloride (6 mg/kg, Xylapan 20 mg/mL). Humidified oxygen was provided via an oxygen mask tightly fitted to the animals, who continued to breathe spontaneously. After induction of anesthesia, venous access was achieved via catheterization of the lateral ear vein (20-ga vascular catheter) for continuous intravenous anesthesia. Fentanyl (1 mg/kg) was added to optimize pain control. The sternohyoid and sternothyroid muscles were infiltrated with lidocaine (6 mg/kg 1%) before dissection. Postoperative pain relief was managed by subcutaneous administration of buprenorphine (0.2 mg/kg, Temgesic) and transdermal fentanyl patches (12 μg/h for 72 hours) (Durogesic matrix, 12 μg/h for $\leq$36 hours after the operation. The animals were under daily clinical observation. Euthanasia was performed after the follow-up MRA under the same anesthesia as previously described, by intra-arterial bolus injection of sodium thiopental (40 mg/kg). Subcutaneous acepromazine (0.005/kg, Prequillan 10 mg/1 mL) was used as neuroleptic/sedative during transportation to the interventional suite.

Surgical Techniques

The animals were fixed in a supine position on an electric heating pad. After extensive neck shaving, a midline incision was made from the manubrium sterni to the angle of the jaw. In the subcutaneous fat tissue between the sternohyoid and sternomastoid muscle, the internal, external, and transverse jugular veins were dissected. Segments of the left external jugular vein or the bifurcation of the jugular vein (internal-external or transverse-external jugular vein) served as grafts for the creation of bilobular, bisaccular, and broad-based aneurysms.

Bilobular Aneurysm. The internal-external or transverse-external jugular vein bifurcation was ligated 5 mm proximal and distal to the bifurcation with 4–0 silk, resected, and kept in a mixture of heparinized (1000 IU, Liquemin 5000 IU/mL) and papaverinized (1 mL, papaverine hydrochloric acid 4%, 40 mg/mL) saline (0.9%, 100 mL) (Fig 1*A*).

Bisaccular Aneurysm. Two 1-cm segments of the left or right external jugular vein were prepared, ligated proximally and distally with 4–0 silk, resected, sutured together (4–5 sutures), and kept in a mixture of heparinized saline and papaverine (Fig 1*B*).

Broad-Neck Aneurysm. A 1-cm segment of the left external jugular vein was dissected, resected, incised along the longitudinal axis, and sutured together at both the proximal (4–5 sutures) and distal (2–3 sutures) ends (Fig 1*C*).

The LCCA was prepared over a distance of approximately 3–4 cm just proximal to the carotid bifurcation. Tiny arterial branches running medially were preserved. The RCCA was isolated and mobilized as far distally and proximally as possible. At this stage, animals received 1000 IU of heparin intravenously. Next, the RCCA was ligated as far proximally as possible and temporarily clipped distally. The vessel was cut as proximally as possible to obtain a long donor artery for a tensionless anastomosis. The exposed LCCA segment was temporarily clipped by using atraumatic clamps. The elliptic arteriotomy was performed according to the size of the prepared complex venous pouch aneurysm.

An anatomic overview of cranial arteries and veins that were involved in aneurysm construction is presented in Fig 2*A*, -*B*, respectively. Before starting the anastomosis procedure, we extensively irrigated all vessels with heparinized saline and papaverine. The vessel adventitia was removed meticulously. The anastomosis procedure that follows does not differ significantly from the conventional venous pouch bifurcation model described elsewhere (Fig 3).[7]

Briefly, the distal end of the RCCA was sutured to the back of the LCCA. The venous pouch was sutured to the back of the RCCA (3–4 sutures) and then anastomosed to the LCCA on the back side (4–5 sutures, 6–8 in case of broad-neck aneurysms) with 10–0 threads (Ethilon; Ethicon, Somerville, New Jersey) (Fig 3*A*, steps 1, 2, and 3). The same procedures were performed on the front side (Fig 3*B*, steps 4, 5, and 6). Before placement of the last frontal stitch, the right clip of the RCCA was removed to allow backflow into the complex aneurysm construction. After prompt filling and washout of trapped air and debris, the last sutures were placed. The suture lines at the aneurysm neck were covered with small pieces of fat tissue to enhance coagulation. During the anastomosis procedure, the vessels were thoroughly and continuously rinsed with papaverine. The skin incision was closed with absorbable threads.

Postoperatively, all animals received intravenous acetylsalicylic acid (10 mg/kg, Aspégic, 500 mg/5 mL), intramuscular vitamin B_{12} (1 mL, 1000-mcg/mL), intravenous antibiotic prophylaxis (0.7 mL/kg, 25-mg/mL Clamoxyl), and glucose infusion (glucose 5%, 60 mL) to compensate for dehydration during surgery. All animals received 250 IU/kg of low-molecular-weight heparin subcutaneously daily for 3 days. Oral acetylsalicylic acid was given daily $\leq$5 weeks postsurgery.

2D-DSA

2D-DSA was performed 3 weeks after the creation of the aneurysms with the rabbits under general anesthesia. The rabbit's left or right femoral artery was microsurgically exposed and cannulated by using a straight 5.5F vascular sheath. The sheath was introduced in a retrograde manner and fixed distally. Images were obtained by rapid sequential 2D-DSA at 2 frames per second by using a small focal spot (BV Pulsera, Philips Medical Systems, Zurich, Switzerland). Anteroposterior and lateral views were obtained (Fig 1*A2*–*C2*). Intra-arterial bolus injection of nonionic iopamidol (0.6-mL/kg Isovue; Bristol-Meyers Squibb, Princeton, New Jersey) as a contrast agent was administered at a rate of approximately 3 mL/s.

CE-3D-MRA

Five weeks after aneurysm creation, animals underwent CE-3D-MRA by using a 1.5T scanner, Magnetom Avanto Syngo B17 (Siemens, Erlangen, Germany). T2-weighted fast spin-echo (TR, 4300 ms; TE, 83 ms; FOV, 137–200 mm; 3-mm section thickness; matrix, 240 $\times$ 512) and 3D-TOF-MRA gradient-echo sequences were performed. To avoid potential overestimations of the aneurysm height, we did not include 3D-TOF-MRA data in the analysis of this preliminary study.[8] After manual bolus injection of gadobutrol (0.1-mL/kg Gadovist; Schering, Berlin, Germany), CE-3D-MRA was performed by using T1-weighted 3D fast-spoiled gradient recalled imaging (TR,

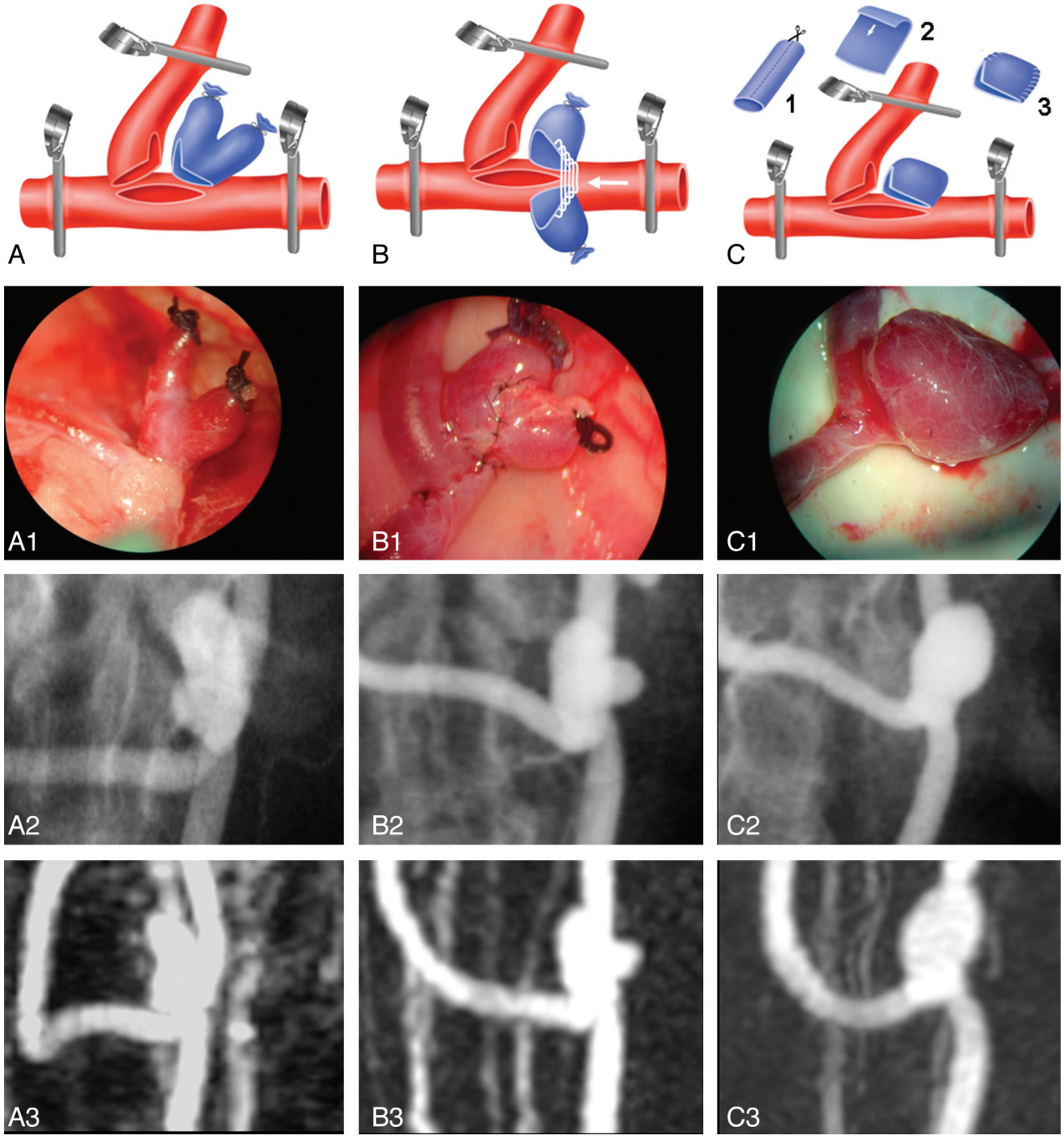

Fig 1. Schematic sketches of surgical steps, (*A–C*), intraoperative photographs under the operating microscope (*A1–C1*), and 2D-DSA (*A2–C2*) as well as CE-3D-MRA (*A3–C3*) screen shots of bilobular, bisaccular, and broad-neck aneurysms. *A*, Bilobular aneurysm. The jugular vein bifurcation stump is anastomosed to the CCA bifurcation, as described in the text and presented in Fig 3. *B*, Bisaccular aneurysm. Two venous pouches of the left or right external jugular vein are sutured together (*white arrow*) and anastomosed to the CCA bifurcation. *C*, Broad-based aneurysm. A 1-cm segment of the left external jugular vein is incised in a longitudinal manner, folded along its transverse axis (1), sutured together proximally (4–5 sutures) and distally (2–3 sutures) (2), and anastomosed to the CCA bifurcation (3).

3.5 ms; TE, 1.3 ms; FOV, 137–200 mm; 1-mm section thickness; matrix, 352 × 512) (Fig 1*A3–C3*).

Morphometric Measurements

2D-DSA measurements, including aneurysm dome (length and width) and aneurysm neck, were performed by using the standardized software installed in the DSA equipment in reference to an external sizing device (Autosuture APPOS UCL 35W stainless steel skin stapler; Covidien, Mansfield, Massachusetts) (Fig 4*A*). The same aneurysm characteristics were measured in CE-3D-MRAs by using the best 3D projections, which included parent vessel and all dimensions of the created aneurysm (Fig 4*B*). To assess morphologic features, we measured each aneurysm 3 times in a blinded fashion by using the automatic measurement tool of the ImagePro Discovery analysis software (Media Cybernetics, Silver Spring, Maryland). Values were expressed as mean ± SD. The volume of the aneurysm was calculated approximately on the basis of a cylindrical volume formula: aneurysm volume = $3.14 \times (\text{width} / 2)^2 \times \text{length}$.[9]

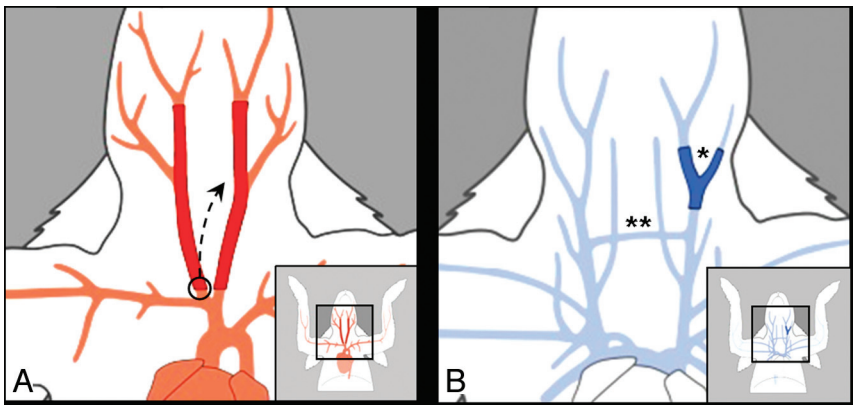

Fig 2. Arterial (red, *A*) and venous (blue, *B*) neck vascular anatomy of the rabbit. *A*, The LCCA is exposed and isolated for a segment of at least 5 cm. The RCCA is dissected distally to its proximal origin at the brachiocephalic trunk (*black circle*) to achieve a tensionless end-to-side anastomosis of the RCCA to the LCCA (*black arrow*). *B*, A 10- to 15-mm segment of the right or left external jugular vein is used for the construction of bisaccluar and broad-neck aneurysms. The internal-external (*asterisk*) or transverse-external (*double asterisks*) jugular vein bifurcation serves as a graft for the creation of bilobular aneurysms.

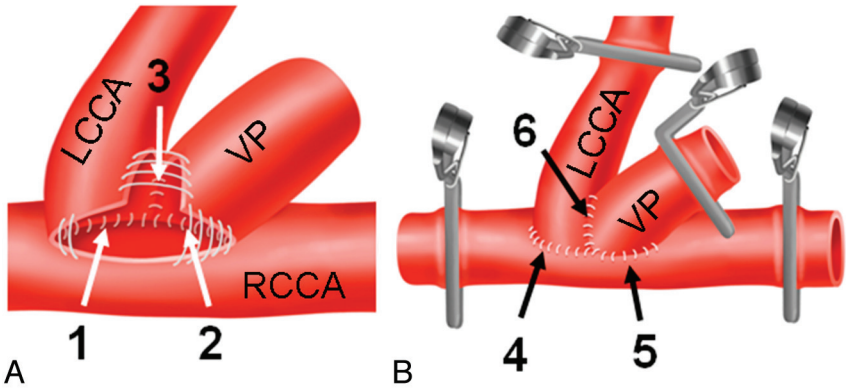

Fig 3. Surgical steps of the conventional microsurgical saccular (berry-shaped) venous pouch bifurcation aneurysm model. *A*, Anastomosis sequences on the back side of the aneurysm (*white arrows*): 1) The LCCA is sutured to the RCCA. 2) The VP is sutured to the RCCA. 3) The VP is sutured to the LCCA. *B*, Anastomosis sequences on the front side of the aneurysm (*black arrows*): 4) The LCCA is sutured to the RCCA. 5) The VP is sutured to the RCCA. 6) The VP is sutured to the LCCA.

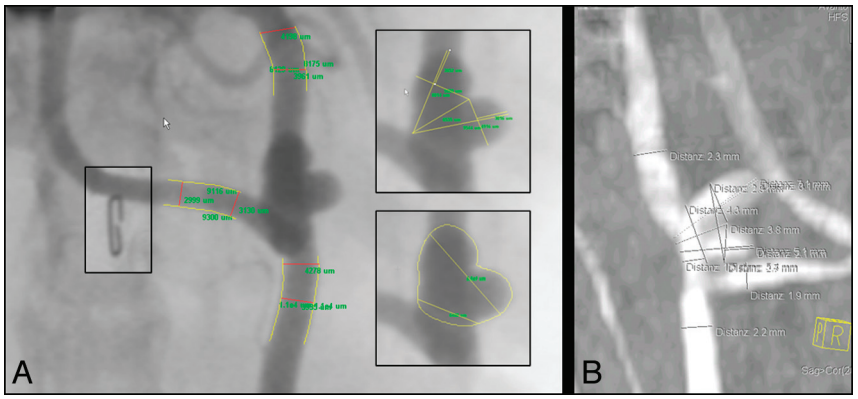

Fig 4. *A*, The screenshots illustrate 2D-DSA measurements, including parent vessels and aneurysm length, width, and neck in reference to an external sizing device (highlighted inset boxes). *B*, The same vessel and aneurysm characteristics are measured in CE-3D-MRA.

Results

Mortality and Morbidity

Perioperative and postoperative mortality was 0%. No postoperative infections and no respiratory, neurologic, or gastrointestinal complications were observed. There was no morbidity except for 1 postoperative hemorrhage at the site of aneurysm creation (morbidity rate, 9%). The animal with the postoperative hemorrhage and the one with a thrombosed aneurysm in the CE-3D-MRA examination were excluded from the morphometric analysis.

Neuroradiologic Findings

There were no technical problems during the performance of 2D-DSA. High-quality imaging of the aneurysms could be obtained in the 2D-DSA projections and CE-3D-MRA (Fig 1 *A*2–*C*2 and *A*3–*C*3). The aneurysm dome (length and width)

Table 1: Surgical characteristics, 2D-DSA, and CE-3D-MRA morphometric measurements

Model/ Modality	No.	Operation Time (min)	No. of Sutures	RCCA (mm)	p-LCCA (mm)	d-LCCA (mm)	Neck Width (mm)	Length/Width Lobule 1 (mm)	Length/Width Lobule 2 (mm)	Volume (mm^3)
BL-2DD	1	155	21				3.5	5.7/3.8	5.1/3.8	122.4
BL-3DM				1.9	2.2	2.3	3.6	5.2/3.8	5.4/3.9	123.7
BL-2DD	2	135	27				4.5	8.2/3.6	5.6/3.4	123.7
BL-3DM				2.8	2.6	2.5	4.4	7.3/3.8	5.7/3.2	128.5
BL-2DD	3	170	22				4.3	7.3/3.5	7/3.9	153.4
BL-3DM				2.8	3.2	2.8	4.5	7.1/3.8	7.3/3.9	169.9
BS-2DD	4	189	28				4	8.4/3.9	9.5/3.5	178.6
BS-3DM				2.4	2.4	2.2	3.9	8.3/3.4	8.9/3.6	165.8
BS-2DD	5	190	31	2.9	3.1	3.5	5.4	8.5/4	8.8/4.9	272.6
BS-3DM				3.1	3.4	3.5	5.3	8.6/4.3	8.9/4.5	266.3
BS-2DD	6	160	28				5.2	8.5/5.2	8.2/4.9	335
BS-3DM				2.7	2.9	2.6	5.3	8.6/5.3	8.3/4.6	327.5
BN-2DD	7	140	26	2.8	3.2	2.7	5.9	5.6/8.1	–/–	199.4
BN-3DM				3	3.2	2.8	5.3	5.2/8.7		184.7
BN-2DD	8	185	32	3	3.4	2.7	9.2	4.3/9.5	–/–	137.9
BN-3DM				3	3.6	2.8	8.9	4.7/10.4		180.3
BN-2DD	9	165	27	2.3	2.4	2.1	7.2	4.8/8.3	–/–	150.1
BN-3DM				2.4	2.3	2.3	7.3	4.3/9.3		235

Table 2: Summary of 2D-DSA and CE-3D-MRA volumes

Model/Modality	No.	Mean Volume (mm^3)
BL-2DD	1–3	133.2 ± 17.5
BL-3DM		140.7 ± 25.4
BS-2DD	4–5	262.1 ± 78.7
BS-3DM		253.2 ± 81.4
BN-2DD	6–9	162.5.1 ± 32.6
BN-3DM		200 ± 30.4

and aneurysm neck could be measured in 9 aneurysms. The 2D-DSA follow-up patency rate at 3 weeks postsurgery was 100%. One broad-neck aneurysm was thrombosed at 5 weeks as shown in the CE-3D-MRA follow-up (patency rate, 91%).

Detailed 2D-DSA and CE-3D-MRA measurements of aneurysm length, aneurysm width, neck width (the bilobular, bisaccular, and broad-neck aneurysms), and the dimensions of parent vessels are given in Table 1. The mean aneurysm volumes measured by using 2D-DSA and CE-3D-MRA sequences are given in Table 2. According to its shape, the broad-neck aneurysm featured the widest neck configuration.

Characteristics of Bilobular, Bisaccular, and Broad-Neck Aneurysm Surgery

The mean operation times were 153 ± 18 minutes, 180 ± 17 minutes, and 163 ± 22 minutes for bilobular, bisaccular, and broad-neck aneurysms, respectively. The overall mean clamping time of both CCAs was 55 ± 12 minutes (range, 45–70 minutes). Tensionless anastomosis of the right CCA to the left CCA was feasible in all animals. The greatest number of interrupted sutures was used to create bisaccular and broad-neck aneurysms, with an average of 29 ± 2 sutures (range, 28–31 sutures) and 28 ± 3 sutures (range, 26–32 sutures), respectively. Fewer sutures (23 ± 3; range, 21–27) were needed to create bilobular aneurysms.

Discussion

This study demonstrates the feasibility of microsurgically creating complex-shaped venous pouch aneurysms without increased incidence of anesthesia-related mortality or procedure-related morbidity and with excellent short-term patency rates. Operation time, clamping time, and average number of sutures did not differ when compared with standard venous pouch bifurcation models.[10,11]

Endovascular embolization in the treatment of large wide-neck cerebral aneurysms, particularly those that are giant or partially thrombosed, remains a challenge.

The range of options for treating cerebral aneurysms has increased, and geometrically difficult aneurysms have recently been tackled by balloon remodeling, endoluminal neck reconstruction devices, self-expandable stents, flow diverters, liquid embolics, and stent-assisted coiling. Due to the improvements in endovascular devices, the previously high aneurysm recanalization rates of wide-neck aneurysms (neck width before treatment >4 mm) are on the decline for the midterm[3,12] but are still unacceptably high for the long term.[1] Animal testing of new devices is inevitable in this constantly changing and fast-growing field. The ability to vary the anatomy of the bifurcation (aneurysm size, neck size, and fundus-to-neck ratio) in microsurgical experimental aneurysm models has been advocated as an advantage over models using elastase-induced aneurysms, in which the size cannot be controlled (though it can potentially be corrected to some degree by adjusting the ligation site).[9,13]

In the present series, we varied not only the shape and size of the arteriotomy but also the geometry of the aneurysm. The surgical techniques result in larger aneurysm volumes (~120–330 mm^3) than are present in conventional berry-shaped venous pouch bifurcation aneurysms (<100 mm^3)[14] or elastase-induced aneurysms (~30–100 mm^3).[9] The created aneurysm necks (~3.5–9.2 mm) are wider than those of conventional microsurgical (~2–3 mm)[14] or elastase-induced (~2.7–3.3 mm) aneurysms.[9]

Despite relatively long operation times of approximately 2.5 hours, the mean clamping time of both CCAs did not exceed 1 hour, which is comparable with conventional surgical aneurysm creation. This indicates that it is not the anastomosis procedure itself but rather the harvest and creation of the venous graft/pouch that requires additional operation time.

This may also explain why the complication rate was not increased despite an increase in operation time. Recently, we facilitated surgical procedures and anesthesia, introduced aggressive anticoagulation therapy, and improved the anesthesia regimen to lower the complication rates and augment the aneurysm patency in the venous-pouch arterial-bifurcation model in rabbits.[7] The modifications in microsurgery and management were adopted in this study, resulting in 0% peri- and postoperative mortality.

Currently, in the clinical setting, the range of cerebral aneurysms found to be suitable for endovascular treatment is steadily increasing. Nevertheless, the incidence of recanalization and recurrent aneurysms after endovascular treatment has to be considered as a limitation of these techniques. The complexity and difficulty of cases demand further development of endovascular technology. The various angioarchitectures of the experimental aneurysm formations presented here offer a promising tool for in vivo animal testing of human devices and a valuable training opportunity for neuroradiologists and endovascular neurosurgeons.

Acknowledgments

We thank Daniel Mettler, DVM, Max Müller, DVM, Daniel Zalokar, and Olgica Beslac, Experimental Surgical Institute, Department of Clinical Research, Bern University Hospital, Bern, Switzerland, for their skillful management of animal care, anesthesia, and operative assistance. Finally, we are especially grateful for the editorial support of Jeannie Wurz, Department of Intensive Care Medicine, Bern University Hospital, Bern, Switzerland, in proofreading the final version of the manuscript.

References

1. Molyneux AJ, Kerr RS, Yu LM, et al. **International Subarachnoid Aneurysm Trial (ISAT) of neurosurgical clipping versus endovascular coiling in 2143 patients with ruptured intracranial aneurysms: a randomised comparison of effects on survival, dependency, seizures, rebleeding, subgroups, and aneurysm occlusion.** *Lancet* 2005;366:809–17
2. Molyneux A, Kerr R, Stratton I, et al. **International Subarachnoid Aneurysm Trial (ISAT) of neurosurgical clipping versus endovascular coiling in 2143 patients with ruptured intracranial aneurysms: a randomised trial.** *Lancet* 2002;360:1267–74
3. Murayama Y, Nien YL, Duckwiler G, et al. **Guglielmi detachable coil embolization of cerebral aneurysms: 11 years' experience.** *J Neurosurg* 2003; 98:959–66
4. Ferns SP, Sprengers ME, van Rooij WJ, et al. **Coiling of intracranial aneurysms: a systematic review on initial occlusion and reopening and retreatment rates.** *Stroke* 2009;40:e523–529
5. Campi A, Ramzi N, Molyneux AJ, et al. **Retreatment of ruptured cerebral aneurysms in patients randomized by coiling or clipping in the International Subarachnoid Aneurysm Trial (ISAT).** *Stroke* 2007;38:1538–44
6. Guglielmi G, Ji C, Massoud TF, et al. **Experimental saccular aneurysms. II. A new model in swine.** *Neuroradiology* 1994;36:547–50
7. Sherif C, Marbacher S, Erhardt S, et al. **Improved microsurgical creation of venous-pouch arterial-bifurcation aneurysms in rabbits**. *AJNR Am J Neuroradiol* 2011;32:165–69
8. Chung TS, Joo JY, Lee SK, et al. **Evaluation of cerebral aneurysms with high-resolution MR angiography using a section-interpolation technique: correlation with digital subtraction angiography**. *AJNR Am J Neuroradiol* 1999;20:229–35
9. Ding YH, Dai D, Danielson MA, et al. **Control of aneurysm volume by adjusting the position of ligation during creation of elastase-induced aneurysms: a prospective study.** *AJNR Am J Neuroradiol* 2007;28:857–59
10. Bavinzski G, al-Schameri A, Killer M, et al. **Experimental bifurcation aneurysm: a model for in vivo evaluation of endovascular techniques.** *Minim Invasive Neurosurg* 1998;41:129–32
11. Spetzger U, Reul J, Weis J, et al. **Microsurgically produced bifurcation aneurysms in a rabbit model for endovascular coil embolization.** *J Neurosurg* 1996;85:488–95
12. Raymond J, Guilbert F, Weill A, et al. **Long-term angiographic recurrences after selective endovascular treatment of aneurysms with detachable coils.** *Stroke* 2003;34:1398–403
13. Ding YH, Dai D, Lewis DA, et al. **Can neck size in elastase-induced aneurysms be controlled? A prospective study**. *AJNR Am J Neuroradiol* 2005;26:2364–67
14. Sherif C, Marbacher S, Fandino J. **High-resolution three-dimensional 3 T magnetic resonance angiography for the evaluation of experimental aneurysm in the rabbit**. *Neurol Res* 2009;31:869–72